

Modelling the long-term evolution of permeability in a full-scale MBR: Statistical approaches



Nicolas Philippe ^{a,*}, Anne-Emmanuelle Stricker ^a, Yvan Racault ^a, Alain Husson ^a,
Mathieu Sperandio ^{b,c,d}, Peter Vanrolleghem ^e

^a Irstea, UR REBX, 50 Avenue de Verdun, F-33612 Cestas CEDEX, France

^b Université de Toulouse, INSA, UPS, INP, LISBP, 135 Avenue de Rangueil, F-31077 Toulouse, France

^c INRA, UMR792 Ingénierie des Systèmes Biologiques et des Procédés, F-31400 Toulouse, France

^d CNRS, UMR5504, F-31400 Toulouse, France

^e modelEAU, Département de génie civil et de génie des eaux, Université Laval, Québec QC G1V 0A6, Canada

HIGHLIGHTS

- We monitored a full-scale membrane bioreactor for one year.
- Six operating variables and three fouling indicators are used.
- SRT, temperature, flux and organic loading are correlated with long-term fouling.
- MLSS and iron additions have a limited impact on long-term fouling.
- Statistical prediction of long-term permeability evolution is attempted.

ARTICLE INFO

Article history:

Received 20 December 2012

Received in revised form 22 April 2013

Accepted 22 April 2013

Available online xxxx

Keywords:

Membrane bioreactor

Full-scale

Fouling

Municipal wastewater

Modelling

ABSTRACT

Even if fouling in membrane bioreactors (MBRs) has been extensively studied during the last decade, its causes and mechanisms are not well understood yet. Furthermore, few full-scale and long-term experiments have been published, and their results do not always match with the models developed from lab-scale studies.

A statistical approach linking long-term and short-term permeability evolution with operational variables in full-scale membrane bioreactors for domestic waste-water treatment is presented. Data originate from a 66,700 P.E. MBR plant monitored for more than one year. Permeability and several fouling indicators were calculated in each of the four hollow-fibre membrane tanks of the plant. The influence of SRT, temperature, MLSS, F:M ratio, iron dosing and membrane flux on daily permeability evolutions, instantaneous permeability evolution and hydraulic backwash efficiency was studied. In order to minimise the bias due to correlations between input variables, a statistical approach using principal component regression and partial least-square regression was tested. Flux, temperature, SRT and F:M ratio are the most influential input variables on long-term permeability evolutions. Iron dose and MLSS are less correlated with fouling indicators. The proposed approach may be improved by integrating the history of the membrane to better describe and predict the permeability evolution.

© 2013 Elsevier B.V. All rights reserved.

1. Introduction

Over the last decade, filtration in membrane bioreactors (MBRs) has been extensively studied since fouling and the related energy consumption to mitigate it are one of the main bottlenecks for the development of this technology [1]. To help filtration design and operation, different models have been proposed and calibrated, essentially based on lab-scale and pilot-scale experiments.

On the one hand, mechanistic models based on physical filtration laws have been proposed. Resistances in series coupled with mass balances are the most common approach [1–5]. Applications of these models have been restricted to relatively short-term periods, mostly in the range of 1 h–10 d and exceptionally up to 65 d. These models contain a large number of parameters and variables, such as sludge supernatant composition and especially soluble microbial products (SMPs) concentration, shear stress, or size distribution of particles and membrane pores. A few other mechanisms have been highlighted in exploratory studies, but they are poorly quantified and formalised in models. Examples include the protection of membranes against deep

* Corresponding author. Tel.: +33 5 57 89 08 00; fax: +33 5 57 89 08 01.

E-mail address: nicolas.philippe@irstea.fr (N. Philippe).

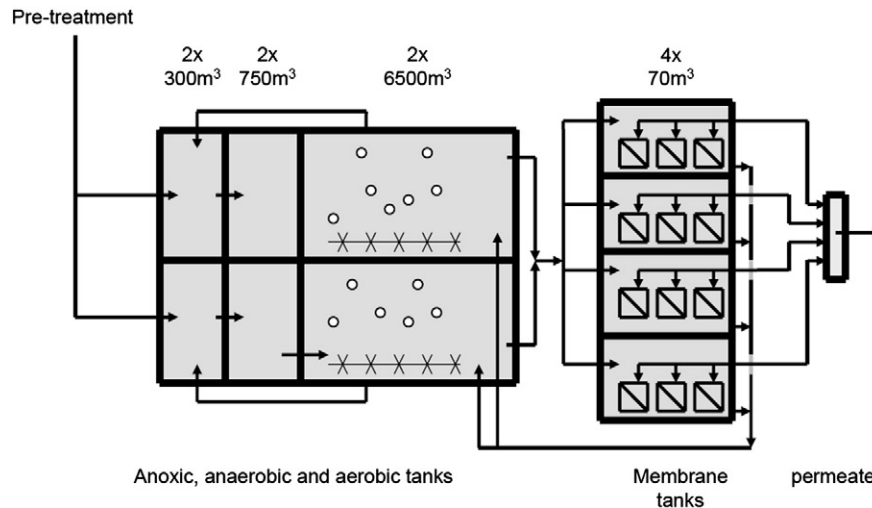


Fig. 1. Simplified MBR layout.

fouling by the cake layer [6], or the role of the nature of SMP (protein/polysaccharides/humic substances) in their ability to attach to the membrane. Many studies highlight polysaccharide predominance in fouling [7–9] but for others, the protein content in the colloidal phase [10,11] or humic substances [12] is the main factor. Since experimental conditions and analysis methodologies differ, comparing these studies can be very complex. Furthermore, they allow to identify mechanisms but not to quantify their contributions to overall fouling.

On the other hand, empirical models based on statistical analysis of data can integrate unknown mechanisms in multivariate linear correlations [13–15].

On full-scale plants, only two of the reviewed studies aim at modelling permeability [16,17]. The model of Wintgens et al. [16] was upgraded and implemented in the GPS-X software by Sarioglu et al. [5] on a long pilot plant monitoring period. The model is based on resistances in series with cake deposition and a mass balance of SMP inside the membrane to make internal fouling increase with the cumulated filtered volume. Cake deposition has an impact only when filtration experiences a process upset. Ludwig et al. [17] use almost the same concepts and obtain good results for transmembrane pressure (TMP) simulation, but only for short periods (1–4 day validation periods). Unlike in most full-scale data found in literature [18], no progressive increase of permeability is modelled in these studies. This is probably because mechanical and chemical cleaning (backwashing, maintenance cleaning) is not, or poorly, accounted for in the models. Also, some of the more complex mechanisms described previously are not considered in models calibrated on large-scale experimental setups. In full-scale MBRs, the limited monitoring of operating conditions doesn't allow this kind of detailed study. A prior statistical analysis between sludge characteristics, operating conditions and fouling may provide a deeper insight into the predominant fouling mechanisms and their respective weights.

The aim of this study is to present a statistical analysis of operational conditions (flux, FeCl_3 dose), sludge characteristics (SRT, F:M ratio, temperature, and MLSS) and fouling indicators. A full-scale MBR with four parallel membrane tanks (MTs) equipped with hollow-fibre membranes was monitored for one year. Appropriate sequences of flux used in pilot-scale membrane bioreactors to characterise fouling are not feasible in full-scale. However the availability of a wide range of flux variations (15 to 50 LMH) in the full-scale plant, even erratic, can be used with appropriate data processing. Three fouling indicators were calculated to get the most information out of full scale data that are not initially designed for fouling characterization in a research context.

First, a principal component analysis (PCA) was conducted on input variables to identify their correlations, and a principal component regression (PCR) was conducted to analyse links between main groups of variables and fouling indicators. Then a partial least square regression (PLSR) was used to highlight which variables or groups of variables are best correlated with these indicators. The prediction ability of these approaches is then discussed and the perspective of improving the models is commented.

2. Materials and methods

2.1. MBR plant description

A MBR plant in the Paris area designed for 66,700 P.E. (Fig. 1) was monitored for one year. The mixed liquor from the two biological

Table 1
Main characteristics and operational variables of the MBR during period 1.

Plant-wide data	Design capacity	66,700 P.E. 10,500 m ³ ·d ⁻¹ 11,100 kg COD·d ⁻¹ 8200 m ³ ·d ⁻¹
	Average influent flow rate	8200 m ³ ·d ⁻¹
	Activated sludge tanks volume (anoxic + anaerobic + aerated tanks)	2 × 7550 m ³
	Membrane tanks volume	4 × 70 m ³
	Pre-treatment	Grit removal, fat removal, sieving 0.8 mm
	SRT	50–70 d
	HRT (for average flow rate)	38 h
Membranes	Membrane type	Hollow fibre ZeeWeed 500d (GE-Zenon)
	Mean pore size	0.04 μm
	Material	PVDF
	Membrane area	4 × 4550 m ²
	Filtration flux	10–50 LMH
	Instantaneous SAD _m	0.62 Nm ³ ·m ⁻² ·h ⁻¹ (50% of the time)
Activated sludge	Average organic loading	4200 kg COD·d ⁻¹
	Average F:M ratio	0.052 kg COD ⁻¹ ·kg MLVSS ⁻¹ ·d ⁻¹
	MLSS (aeration tanks)	5–9 g·L ⁻¹
	MLSS (membrane tanks)	6–10 g·L ⁻¹
	MLVSS	4.5–6 g·L ⁻¹
	Temperature	10–21 °C
	Average iron dose	Winter: 90 kg Fe·d ⁻¹ (8.8 mg Fe/L _{influent}) Summer: 140 kg Fe·d ⁻¹ (18 mg Fe/L _{influent})

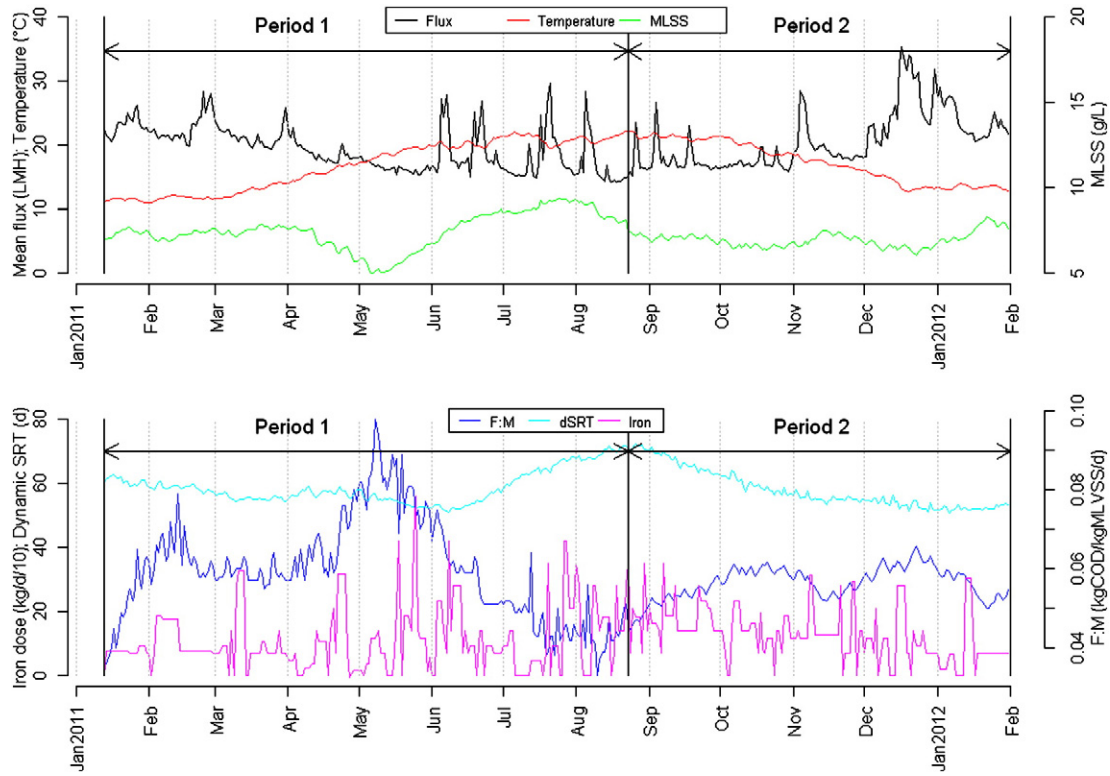


Fig. 2. Input variables trend over the whole monitoring period.

treatment trains (anoxic, anaerobic and alternating aerobic/anoxic tanks) is mixed and then filtered by hollow fibre modules (Zeeweed 500d, Zenon) installed in four separate membrane tanks (MTs). Their air flow rate could not be measured directly, but it was very likely identical since the air blowers were identical and independent for the 4 MTs. Furthermore measured power consumption was the same four all 4 blower engines. The cyclic air flow rate (10 s on/10 s off) was constant during the whole monitoring period. The specific aeration demand per membrane area (SAD_m) is $0.62 \text{ Nm}^3 \cdot \text{m}^{-2} \cdot \text{h}^{-1}$ when aeration is on. Filtration is sequenced as follows: 10 min

filtration/1 min backwash, with maintenance cleanings (short chemical cleanings with bleach and citric acid) every 3 or 4 d. The main plant data are summarized in Table 1.

The monitoring period was split into two periods. During period 1 (January 13 to August 23, 2011), additional online sensors were set up in the influent and permeate streams to monitor COD and nitrogen (NH_4, NO_3) (S:CAN, Messtechnik GmbH, Austria; Hach Lange, Germany), and in the biological tanks to monitor MLSS, DO and pH. Almost twice a week sampling enhanced the setup for probe calibration and additional analyses ($\text{BOD}_5, \text{TKN}, \text{NO}_2, \text{TP}, \text{PO}_4$). The samples were analysed using

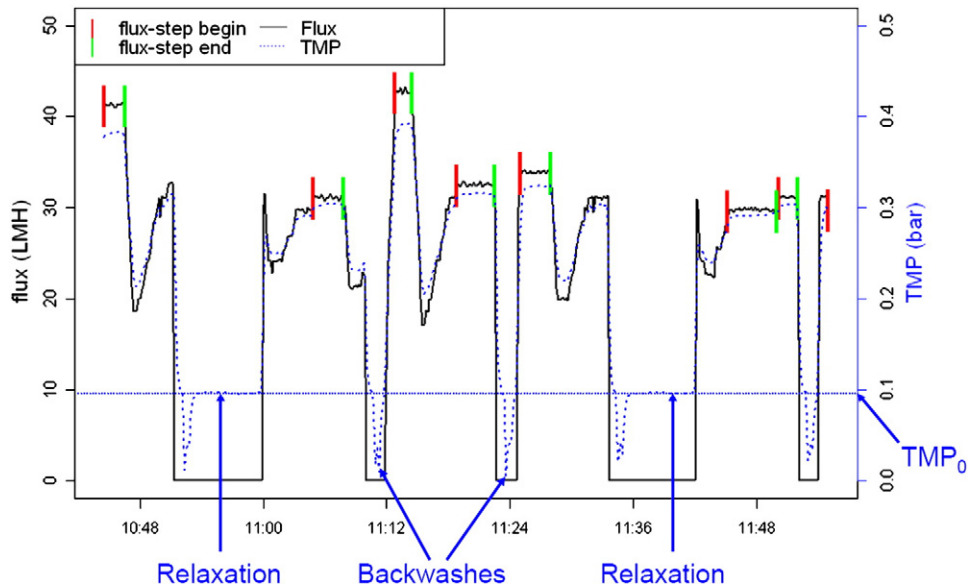


Fig. 3. Example of flux and TMP variations over 5 filtration cycles.

the French or European standard methods (NF-EN) in the Irstea laboratory, and on site using rapid test kits (Hach Lange, Germany). The plant's existing data acquisition system provided flow rates, transmembrane pressure, temperature, sludge wastage and equipment operation logs. The protein and polysaccharide contents of influent wastewater, sludge supernatant and permeate were analysed at the beginning of period 1. The limit of quantification for protein and polysaccharides in our lab was respectively $5 \text{ mg BSA} \cdot \text{L}^{-1}$ and $10 \text{ mg Glucose} \cdot \text{L}^{-1}$, based on error on standard solution of BSA and Glucose <20%. The concentrations found in sludge supernatant and permeate were near $10 \text{ mg BSA} \cdot \text{L}^{-1}$ (protein) and below $5 \text{ mg Glucose} \cdot \text{L}^{-1}$ (polysaccharides). These low values incited us to give up measuring this variable. The low concentration may be explained by the long SRT above 50 d [19] and/or the high iron dose that could help flocculation and chelating of SMP [20].

During period 2 (August 23, 2011 to January 31, 2012), a fraction of the online probes had been removed. Influent, permeate and sludge monitoring were limited to routine operation analysis conducted about twice a week (24-h composite samples for influent and permeate, and grab samples in aeration tanks for dry matter analysis). The results for period 2 were corrected if necessary according to correlations between lab-measurement and operator measurements made during period 1.

2.2. Variations of the main operational variables

Operational variables selected to characterise the sludge are temperature, MLSS, F:M ratio, SRT, and iron dose. These variables are plotted in Fig. 2. They have been chosen because they are available to operators, which is a prerequisite for potential application of our method. pH and MLVSS (63–73% MLSS) were also available but not used in this study since they were respectively quite stable (7.0–7.6) and too much correlated with MLSS.

Since SRT varied strongly during the monitoring period, it was calculated dynamically using the method of Takács et al. [21], to better represent the real floc retention time, according to the following equation:

$$d\text{SRT}_d = d\text{SRT}_{d-1} + 1 - \frac{\text{SRT}_{d-1} \cdot F_p}{M_d} \quad (1)$$

where M_d is the total solids mass in the whole plant (kg) and F_p is the daily sludge production (kg). F_p was calculated by two means in order to ensure the reliability of the results. On the one hand F_p was calculated as the product of a solids production yield (Y_{SP}) and influent COD load. Average Y_{SP} was calculated as the slope of cumulated solids balance and influent COD load, and validated using a COD balance over the whole plant [22]. On the other hand F_p was calculated with the volume and concentration of wasted sludge and validated versus the weight of hauled dewatered solids. There are no differences in this calculation between the two periods, but in raw data used. Sludge production calculation during period 1 was based on our own sensors and analysis, whereas during the period 2, it was based on operators' data. Sludge production yield calculated during the second period is still in agreement with the results available when MLSS and COD balances were performed over the whole plant.

The iron chloride dose added into the anoxic tanks for enhanced phosphorus removal was quite high (Table 1) to comply with stringent effluent quality requirements, especially in the summertime ($0.4 \text{ mg TP} \cdot \text{L}^{-1}$ during the low water period in the receiving stream). Upsets of the iron chloride dosing pumps explain the sudden dose variations seen in Fig. 2. High variations of MLSS between April and July 2012 (Fig. 2) were performed intentionally for the study by increase/decrease of sludge wastage.

2.3. Permeability calculation

For each MT, the permeate flux and TMP are recorded every 10 s. Due to a complex flux automation system to control the water level in

the MTs, flux and TMP fluctuate a lot. The flux can vary between 10 and 50 LMH within the same filtration cycle. An example of these variations is presented in Fig. 3. A programme has been developed with the R language (R Development Core Team, 2009) to isolate stable flux-steps and remove TMP stabilisation phases. About 20% of the total filtration time could finally be selected for permeability calculations. Permeability (L_p) was calculated with corrections for (i) temperature, (ii) head loss in permeate pipes, and (iii) pressure sensor drift, using the following equation:

$$L_p = \frac{\mu_p}{\mu_p^{20}} \cdot \frac{J}{\text{TMP}_{\text{measure}} - \text{TMP}_0 - \alpha J^2 L_{\text{tube}}} \quad (2)$$

where J is the membrane flux, α the head-loss coefficient, L_{tube} the tube length between membrane modules and pressure sensors, and μ_p and μ_p^{20} are respectively the permeate viscosity at temperature T assuming Eq. (3) [1] and at 20°C (water viscosity). TMP_0 is the residual pressure measured by the TMP sensor during relaxation phases that last more than 10 min, and averaged on 5 d.

$$\mu_p = \mu_p^{20} \cdot 1.78 e^{-0.041 T^{0.875}} \quad (3)$$

After these corrections, the instantaneous permeability is no longer affected by the instantaneous flux, which tends to reject hypothesis about filtration mechanisms that depend instantly on flux (cake compressibility and concentration polarisation) (see Section 3.3).

2.4. Fouling indicator calculation

Due to the particular behaviour of flux, specific fouling indicators were developed for this WWTP. Even if it doesn't allow dissociating properly between different fouling types like with some dedicated flux-step sequencing strategy used in pilot-scale studies, it is an attempt to get the most information out of these full-scale data. The indicators are calculated based on the corrected permeability as presented in Section 2.3. It was chosen because it doesn't depend on instantaneous fluxes which presented lots of variations, and represents well the fouling status of membranes.

Two short-term (2–10 min) and one mid-term (one day) fouling indicator have been defined and calculated:

- iBW (impact of hydraulic backwashes on permeability): when permeability can be calculated less than 2 min before and after a backwash sequence (at least 40 s stable flux-step each side), the difference between the two values is an indicator of the backwash efficiency. iBW is then calculated as the daily average of this

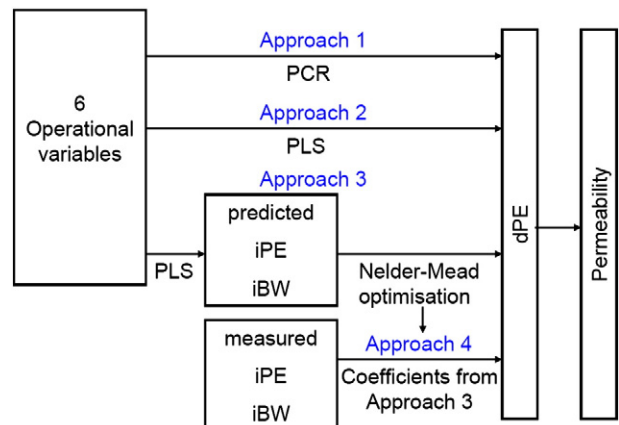


Fig. 4. Overview of the four statistical approaches.

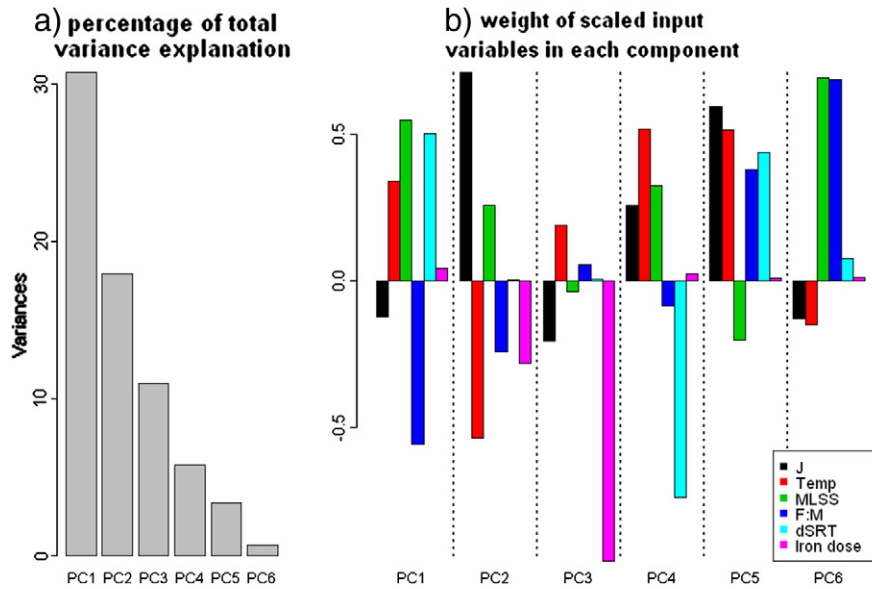


Fig. 5. (a) Contribution of each principal component to the total variance of the input dataset. (b) Composition of each component in terms of scaled input variables.

indicator (in $\text{LMH}\cdot\text{bar}^{-1}$). It represents a part of the physically reversible fouling, which may include both surface and internal deposits.

- iPE (instantaneous permeability evolution): on each flux-step, a time-linear regression is performed on permeability. iPE is then calculated as the daily average of the permeability slopes (in $\text{LMH}\cdot\text{bar}^{-1}\cdot\text{s}^{-1}$). It represents short-term (about 1–9 min) fouling, often associated in literature with particles deposition on membrane surface.
- dPE (daily permeability evolution): dPE is the difference between the average permeability of day d minus that of day $d - 1$ (in $\text{LMH}\cdot\text{bar}^{-1}$). It represents a numerical derivative of the long-term permeability drift.

2.5. Statistical modelling of permeability

The aim of the study was to link the fouling indicators defined above to operational variables. In the rest of the paper, operational variables refer to flux, temperature, MLSS, F:M ratio, dSRT and Iron dose.

A statistical multivariate analysis was performed to highlight correlations between different elements: (i) daily operational variables themselves, (ii) daily operational variables and dPE, (iii) operational variables and short-term fouling indicators (iBW and iPE), and (iv) short-term fouling indicators (measured or predicted) and dPE.

Two types of regressions were used: Principal Components Regression (PCR) and Partial Least Square Regression (PLSR). Their advantage, especially for PLSR, is that they allow determining independent effects of each input variable even if they are correlated.

Table 2

Pearson correlation matrix between operational variables (significant correlations are bolded).

	Flux	Temperature	MLSS	F:M	dSRT	Iron dose
Flux	1.00					
Temperature	-0.63	1.00				
MLSS	-0.02	0.19	1.00			
F:M	-0.02	-0.17	-0.75	1.00		
dSRT	-0.37	0.52	0.38	-0.54	1.00	
Iron dose	-0.17	0.23	-0.04	-0.03	0.17	1.00

PCR aims at defining components (linear combinations of input variables) that are both uncorrelated and represent the maximum of the total variance of input variables. It highlights correlations between the original input variables. A linear regression between one or several of these components and output variables is then performed.

PLSR is the same type of regression, but differs in the construction of components: instead of maximising only the total variance of input variables, PLSR aims to maximise the combined variance of input and output variables, which improves the prediction ability for output variables.

To apply these methods to our data, four approaches have been used (Fig. 4):

The first two approaches aim at highlighting correlations between operational variables themselves and between operational variables and the long-term fouling indicator (dPE).

Approach 1: a PCA is used to study input variable correlations, and the associated PCR links dPE with the resulting principal components.

Approach 2: PLSR is used to fit dPE, but it uses a different set of input components for each output dataset (i.e. for each of the four MT). Approaches 3 and 4 aim at investigating fouling mechanisms. They highlight links between input variables, short-term permeability evolutions (iPEs), fouling reversibility by backwashes (iBWs) and long-term permeability evolutions (dPEs).

Approach 3: PLSR is fitted to predict instantaneous permeability evolution (iPE) and reversibility (iBW) based on operational variables. The couple of parameters weighting iPE and iBW in a bilinear relationship to predict dPE is then optimized with a Nelder–Mead algorithm.

Approach 4: dPE is calculated directly from a linear combination of the measured values of iPE and iBW using the parameters optimized in approach 3. It is a kind of validation of approach 3.

In approaches 1 to 3, input variables are the 6 operational variables, whereas in approach 4, input variables are the two short-term fouling indicators.

All four approaches yield a linear relationship (Eq. (4)) between operational variables (approaches 1 and 2) or short-term fouling indicators (approaches 3 and 4) and daily permeability evolutions:

$$dPE = L_{p,d+1} - L_{p,d} = \sum a_i \cdot X_i \quad (4)$$

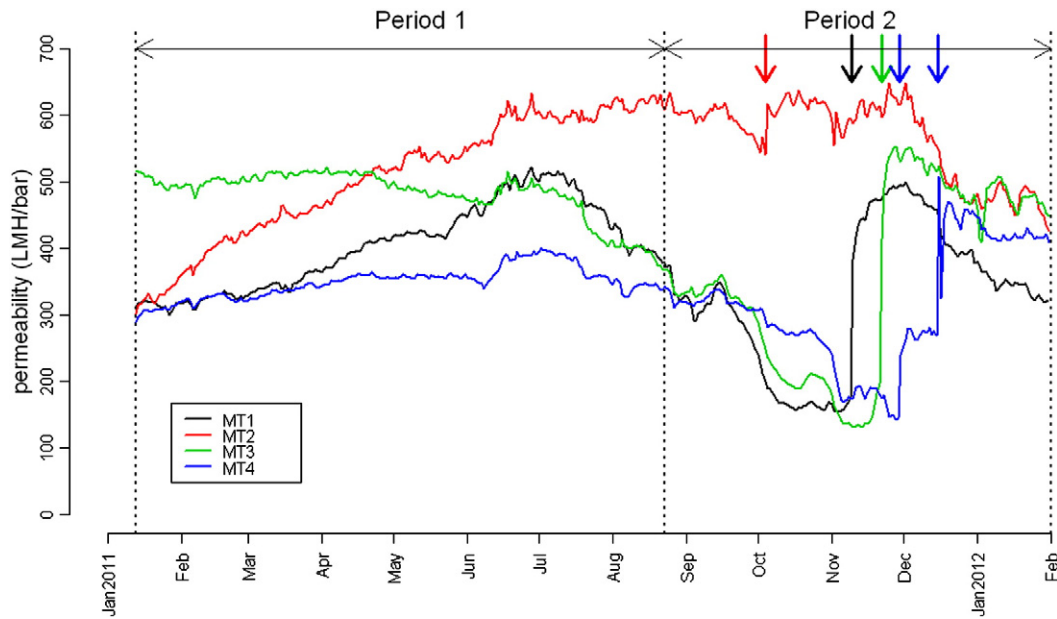


Fig. 6. Permeability evolution over one year in the four membrane tanks. Vertical arrows represent regeneration cleaning.

where a_i is the regression coefficients and X_i the operational variables (approaches 1 and 2) or the short term fouling indicators (approaches 3 and 4).

The value of daily permeability evolution (dPE) obtained from Eq. (3) is then used to calculate the daily average permeability (L_p) using a numerical integration with a one-day time step. L_p is initialized to its measured value at $d = 0$ and after each regeneration cleaning. That way, all four approaches can eventually estimate the long-term evolution of permeability.

Correlation tests between predicted and measured values of dPE, iPE, and iBW yield very low correlation coefficients ($R^2 \leq 0.3$) due to the scatter of measured data. To assess the efficiency of the four statistical methods, the relative mean square error between the predicted and measured daily average permeability was preferred (Eq. (4)):

$$rRMSE = \sqrt{\frac{\sum_i (L_{p,m} - L_{p,p})^2}{\sum_i (L_{p,m})^2}} \quad (5)$$

where $L_{p,m}$ ($\text{LMH} \cdot \text{bar}^{-1}$) is the measured value for daily average permeability, $L_{p,p}$ ($\text{LMH} \cdot \text{bar}^{-1}$) is the predicted value and n the number of days considered.

It allows comparing the four methods in a fair manner, even if their predicted variables are not the same. Calibration of the model was done with the data of period 1 (210 d) and validation with those of period 2 (174 d).

Table 3
Permeability values in other hollow-fibre full-scale studies.

Reference	Permeability range ($\text{LMH} \cdot \text{bar}^{-1}$)	Membrane type
[23]	100–280	Zenon Zeeweed 500c
[18]	200–480	Zenon ZeeWeed 500d
[24]	150–200	Zenon ZeeWeed 500c and 500d
[25]	60–160	Zenon ZeeWeed 500c
[26]	100–250	Zenon ZeeWeed 500c
[16]	60–370	Zenon ZeeWeed ??
Present study	150–600	Zenon ZeeWeed 500d

3. Results

3.1. Correlations between input variables

One of the by-products of approach 1 is an overview of input variable correlations. The first component (PC1) mainly represents sludge characteristics (F:M ratio, dynamic SRT, MLSS and to a smaller extent, temperature). It accounts for 30% of the total variance of operational variables (Fig. 5). The second component (PC2) represents mainly flux and temperature, which are fortuitously negatively correlated: the highest flow rates occur in the winter time due to the rainfall pattern, whereas the flow rates decrease in the summer time due to a reduced population during the holiday season. The third component represents mainly the iron dose, that is quasi independent from other variables. These results show the strong correlations between input variables, which are also illustrated by the Pearson correlation matrix shown in Table 2. SRT is typically strongly correlated with F:M. In our case, the correlation is weaker because variations of MLSS and F:M ratio occurred and SRT was calculated dynamically. As a result, variations of SRT were delayed and smoothed compared to those of MLSS and F:M.

The observed correlations justify the use of PLSR, an appropriate method to dissociate correlated variables in the input dataset, to obtain a descriptive model for the fouling indicators.

3.2. Long-term permeability evolution

Permeability varied over a large range within a year, between 130 and 650 $\text{LMH} \cdot \text{bar}^{-1}$ (Fig. 6). Surprisingly there are significant differences between the behaviour of the four MTs, even though they were filtering the same sludge and their configuration and operating conditions were almost identical (except for MT4 that received a 20–40% lower flux than the other MTs). The most likely reason is heterogeneity of the air flow scouring efficiency in the different membrane tanks. The permeability in MT3 was initially higher because a regeneration cleaning was performed in December 2010. The reason why the permeability in MT2 didn't decrease between July and September 2011 like in the other 3 tanks remains unknown. The efficiency of air scouring in this tank could possibly be better than in the others.

However, like in other full-scale studies, the main trend was that corrected permeability is higher in the summer time and lower in the winter time [18].

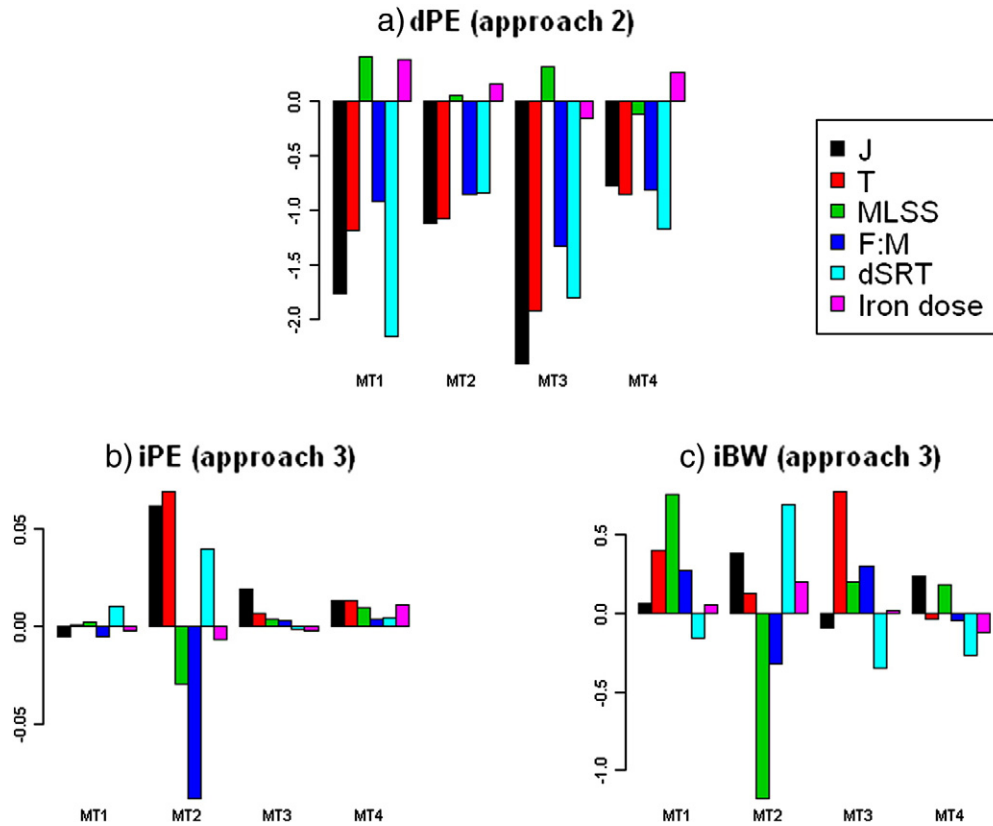


Fig. 7. Contribution of the input variables in the PLS regression for the three fouling indicators.

Another point to be highlighted is that permeability values corrected according to Eq. (2) are very high compared to other studies with the same type of membranes (Table 3). This may be explained by several specific features of the studied plant: (i) the low SMP concentration found at the beginning of the study and confirmed by the good sludge filterability found in a parallel study, and (ii) the small size of the membrane tanks, that implies a high specific scouring aeration density per unit tank volume, even if the specific aeration density per membrane surface area was in the usual range. Another hypothesis is that the permeability calculated in other studies may not have been corrected for pressure sensor drift and head-loss in permeate tubes.

3.3. Influence of operational variables on fouling indicators

The contribution of operational variables to dPE identified with a PLSR is shown in Fig. 7(a). Among the input variables the flux is as expected the main contributor to permeability decrease. It is closely followed by dynamic SRT, temperature and F:M ratio. SRT is often highlighted to be inversely correlated with SMP and thus to membrane fouling. But in most studies, its variation range is 10–40 d [9]. It has already been related that above 50 d as in the studied plant,

the correlation between SRT and SMP concentration [27–29] or their fouling potential [9] is less clear or even reversed.

Temperature impacts several sludge characteristics (viscosity, biological and chemical kinetics, chelating balances) that potentially influence fouling in both ways. For example Miyoshi et al. [11] found a positive correlation between temperature and fouling, whereas some contradictory results were found elsewhere [30]. Other studies highlight the influence of rapid temperature variations instead of its absolute value [31]. Therefore there is no predominant trend in literature.

MLSS seems to be a weak contributor to permeability increase in its variation range (6–10 g·L⁻¹). Iron dose is also a weak contributor to permeability increase whereas it is highlighted to be a filterability enhancer at similar doses in other studies [32,33]. The trend is similar in all four MTs. The role of suspended solids in membrane fouling seems more correlated to its composition (influenced by F:M ratio and SRT) than to its concentration.

Before presenting links between operational variables and short-term fouling indicators, it has to be mentioned that values of iPE and iBW are low compared to their precision. It confirms that fast fouling kinetics are weak. This may mean weak cake formation and compressibility inside a filtration cycle, and weak concentration polarisation. This is probably due to a very high critical flux, above 50 LMH. It confirms that the weak instantaneous relationship between flux and permeability allows us to use permeability as a variable to analyse fouling (see Section 2.3). It also explains partly the poor links between operational variables and the short-term indicators. Nevertheless, some trends can be highlighted in Fig. 7(b) and (c). The four MTs show clear divergence, the contribution of input variables on these indicators, especially on iBW, can even be opposite between the membrane tanks, suggesting different short-term fouling behaviours in each MT. If we only consider the variables for which the contribution is significant, it appears that flux, temperature and SRT seem to increase instantaneous fouling (iPE), while the F:M

Table 4
Relative mean square errors between calculated and measured permeability on period 1.

	Approach 1	Approach 2	Approach 3	Approach 4
MT1	2.94	2.94	4.44	4.45
MT2	7.88	5.11	4.88	5.76
MT3	5.49	3.61	11.18	11.56
MT4	3.09	3.62	3.37	4.33

Table 5

Relative mean square errors between calculated and measured permeability for the validation period, before and after regeneration cleaning.

	Approach 1		Approach 2		Approach 3		Approach 4	
	Before cleaning	After cleaning						
MT1	77.4	32.9	22.1	52.5	47.0	32.5	26.7	25.8
MT2	6.5	51.6	7.0	37.3	13.9	57.6	8.9	54.1
MT3	69.9	28.3	13.9	26.4	133.8	32.7	149.5	36.7
MT4	49.7	18.6	40.9	20.3	26.0	16.4	68.6	NA ^a

Bold numbers refer to most relevant approach for each membrane tank.

^a Inconsistent TMP sensor data.

ratio tends to diminish it. The only clear trend that can be highlighted for iBW is that the reversibility of short-term fouling is positively correlated with the mean flux and temperature.

3.4. Statistical modelling of permeability

This part shows results for the prediction of long-term permeability evolution by the different statistical approaches. Results from the 2 types of approaches will be presented separately: Ap. 1 and 2 (that links directly operational variables and dPE) and Ap. 3 and 4 (that determine relevance of links between short-term and long-term fouling).

Among the first type of approaches, approach 2 is more relevant than approach 1 for both calibration (Table 4) and validation period (Table 5) because the set of variables and parameters used to model dPE is built taking into account the maximisation of dPE variance representation. Thus, only the results of approach 2 will be discussed (1st column in Fig. 8).

Among the second type of approaches, approach 4 seems more relevant than approach 3. In approach 3, the uncertainty of dPE modelling combine the uncertainty of prediction of short-term indicators and that of prediction of dPE (Table 5). Whereas approach 4 is based only on the prediction of dPE with measured short-term indicators. As a result only the results of approach 4 will be discussed (2nd column in Fig. 8).

Furthermore, three categories of MT have to be distinguished: MTs 1 and 2 (that present large permeability evolution starting at a low level); MT3 (permeability starting at a high level due to a regeneration cleaning performed two months before the beginning of calibration period); MT4 (low permeability variations during the whole

calibration period). The results on MT4 won't be further discussed because the weak variations of permeability during period 1 don't allow proper calibration of the model.

Approach 2 seems to predict properly long-term trends on permeability only before regeneration cleaning on MTs 1 and 2, and even after regeneration cleaning on MT3, certainly because it was calibrated not long after a regeneration cleaning only in this tank.

Before regeneration cleaning, approach 4 is far less relevant on MT3 than on MTs 1 and 2, suggesting that long-term permeability evolution is more driven by short-term mechanisms when initial permeability is low. That phenomenon can be explained by the following assumption: fibre network clogging (that was minimised on MT3 by the recent regeneration cleaning) can lead to a higher local flux, and would increase irremovable fouling due to short-term mechanisms by strengthening cake ability to resist physical cleaning and scouring [34].

To conclude this part, two main assumptions will be highlighted:

- When a sudden change in membrane status occurs, models have to be recalibrated.
- Short-term fouling seems to be less removable (and thus a more relevant driving force for long-term fouling) when membrane has not been intensively cleaned for several months.

4. Conclusion

A statistical analysis was performed to highlight the relevance of six conventional variables that can be monitored using standard WWTP instrumentation and sampling on three fouling indicators (one long-term and two short-term).

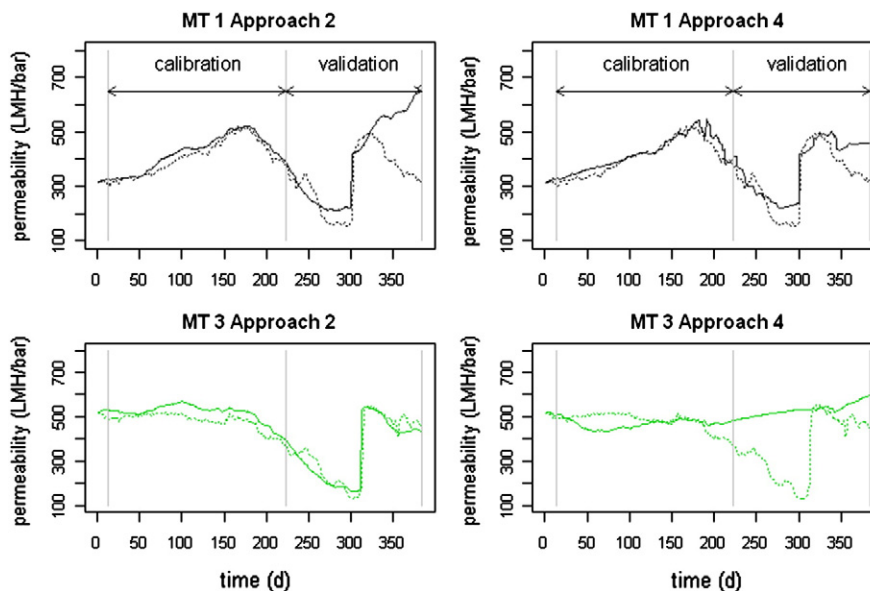


Fig. 8. Predicted and measured permeability values in the MTs 1 and 3 using the approaches 2 and 4. Permeability was reinitialized the day after regeneration cleaning to its measured value.

Flux was the main factor that impacted long-term fouling in our study. Other variables that increase fouling were temperature, F:M and SRT. Iron dose and MLSS were poorly correlated with long-term permeability evolutions.

The link between short-term and long-term evolutions of fouling seems to depend strongly on the initial fouling state of membranes and other differences between membrane tanks that are unknown.

Linking long-term permeability evolutions with the considered operational variables seems successful for a period of several months, but may become less reliable after a regeneration cleaning.

A statistical approach that integrates the history of membrane cleanings, continuous calibration, new input variables or interrelationships between several of the input variables could help to better understand and predict filtration behaviour. Such an approach could help plant operators in their management of operational variables and regeneration cleaning planning.

Acknowledgements

The authors would like to thank the plant operators for their collaboration, and the Irstea technical team (Jean-Claude Gregoire, Jacky Vedrenne, Flavien Beaudoin and Morgane Aubey), as well as the Irstea chemical analysis laboratory staff. Peter Vanrolleghem holds the Canada Research Chair in Water Quality Modelling.

References

- [1] J. Busch, A. Cruse, W. Marquardt, Modeling submerged hollow-fiber membrane filtration for wastewater treatment, *J. Membr. Sci.* 288 (1–2) (2007) 94–111.
- [2] X.-Y. Li, X.-M. Wang, Modelling of membrane fouling in a submerged membrane bioreactor, *J. Membr. Sci.* 278 (1–2) (2006) 151–161.
- [3] T. Jiang, M.D. Kennedy, C. Yoo, I. Nopens, W. van der Meer, H. Futselaar, J.C. Schippers, P.A. Vanrolleghem, Controlling submicron particle deposition in a side-stream membrane bioreactor: a theoretical hydrodynamic modelling approach incorporating energy consumption, *J. Membr. Sci.* 297 (2007) 141–151.
- [4] G. Mannina, G.D. Bella, G. Viviani, An integrated model for biological and physical process simulation in membrane bioreactors (mbrs), *J. Membr. Sci.* 376 (1–2) (2011) 56–69.
- [5] M. Sarioglu, G. Insel, D. Orhon, Dynamic in-series resistance modeling and analysis of a submerged membrane bioreactor using a novel filtration mode, *Desalination* 285 (2012) 285–294.
- [6] J. Wu, C. He, Y. Zhang, Modeling membrane fouling in a submerged membrane bioreactor by considering the role of solid, colloidal and soluble components, *J. Membr. Sci.* vol. 397–398 (2012) 102–111, (cited By, since 1996 1).
- [7] S. Arabi, G. Nakhla, Characterization of foulants in conventional and simultaneous nitrification and denitrification membrane bioreactors, *Sep. Purif. Technol.* 69 (2009) 153–160.
- [8] T. De La Torre, B. Lesjean, A. Drews, M. Kraume, Monitoring of transparent exopolymer particles (TEP) in a membrane bioreactor (MBR) and correlation with other fouling indicators, *Water Sci. Technol.* 58 (2008) 1903–1909.
- [9] S. Liang, C. Liu, L. Song, Soluble microbial products in membrane bioreactor operation: behaviors, characteristics, and fouling potential, *Water Res.* 41 (1) (2007) 95–101.
- [10] M. Hernandez Rojas, R. Van Kaam, S. Schetrite, C. Albasi, Role and variations of supernatant compounds in submerged membrane bioreactors fouling, *Desalination* 179 (2005) 95–107.
- [11] T. Miyoshi, T. Tsuyuhara, R. Ogyu, K. Kimura, Y. Watanabe, Seasonal variation in membrane fouling in membrane bioreactors (MBRs) treating municipal wastewater, *Water Res.* 43 (2009) 5109–5118.
- [12] F. Fan, H. Zhou, H. Husain, Identification of wastewater sludge characteristics to predict critical flux for membrane bioreactor processes, *Water Res.* 40 (2006) 205–212.
- [13] N. Jang, X. Ren, J. Cho, I. Kim, Steady-state modeling of bio-fouling potentials with respect to the biological kinetics in the submerged membrane bioreactor (smbr), *J. Membr. Sci.* 284 (1–2) (2006) 352–360.
- [14] Y. Tian, L. Chen, S. Zhang, C. Cao, S. Zhang, Correlating membrane fouling with sludge characteristics in membrane bioreactors: an especial interest in EPS and sludge morphology analysis, *Bioresour. Technol.* 102 (19) (2011) 8820–8827.
- [15] C. Galinha, G.b. Carvalho, C. Portugal, G.d. Guglielmi, M. Reis, J. Crespo, Multivariate statistically-based modelling of a membrane bioreactor for wastewater treatment using 2d fluorescence monitoring data, *Water Res.* 46 (no. 11) (2012) 3623–3636.
- [16] T. Wintgens, J. Rosen, T. Melin, C. Brepols, K. Drensla, N. Engelhardt, Modelling of a membrane bioreactor system for municipal wastewater treatment, *J. Membr. Sci.* 216 (2003) 55–65.
- [17] T. Ludwig, D. Gaida, C. Keyzers, J. Pinnekamp, M. Bongards, P. Kern, C. Wolf, A.L.S. Brito, An advanced simulation model for membrane bioreactors: development, calibration and validation, *Water Sci. Technol.* 66 (7) (2012) 1384–1391.
- [18] A. van Bentem, N. Nijman, P. Schyns, C. Petri, Mbr Varsseveld: 3 years of operational experience, *Water Pract. Technol.* 5 (2010) 1.
- [19] A. Masse, M. Sperandio, C. Cabassud, Comparison of sludge characteristics and performance of a submerged membrane bioreactor and an activated sludge process at high solids retention time, *Water Res.* 40 (2006) 2405–2415.
- [20] I. Mishima, J. Nakajima, Control of membrane fouling in membrane bioreactors process by coagulant addition, *Water Sci. Technol.* 57 (7) (2009) 1255–1262.
- [21] I. Takacs, A.-E. Stricker, S. Achleitner, A. Barrie, W. Rauch, S. Murthy, Do you know your sludge age, *Proceedings 81st Annual WEF Conference and Exposition (WEFTEC2008)*, vol. 2008, 2008, pp. 3639–3655.
- [22] Y. Racault, S. Gillot, Use of mass balances for the determination of oxygen contribution of the different air sources in a full-scale membrane bioreactor, *Proceedings 80th Annual WEF Conference and Exposition (WEFTEC2007)*, WEF, San Diego, USA, 2007, pp. 3393–3406.
- [23] S. Lyko, T. Wintgens, D. Al-Halbouni, S. Baumgarten, D. Tacke, K. Drensla, A. Janot, W. Dott, J. Pinnekamp, T. Melin, Long-term monitoring of a full scale municipal membrane bioreactor – characterisation of foulants and operational performance, *J. Membr. Sci.* 317 (2008) 78–87.
- [24] C. Brepols, K. Drensla, T. Janot, T. Engels, N. Engelhardt, Performance improvement of full scale membrane bioreactors, IWA Regional Conference an Exhibition on Membrane technology and Water Reuse, Istanbul-Turkey, 2010.
- [25] A. Garcés, W. De Wilde, C. Thoeys, G. De Gueldre, Operational cost optimisation of MBR Schilde, 4th IWA International Membranes Conference: Membranes for Water and Wastewater Treatment (United Kingdom), 2007.
- [26] W. Engelhardt, N. Lindner, Experiences with the world's largest municipal waste water treatment plant using membrane technology, *Water Pract. Technol.* 7–1 (2006).
- [27] W. Chen, J. Liu, F. Xie, Identification of the moderate SRT for reliable operation in MBR, *Desalination* 286 (2012) 263–267.
- [28] F. Meng, S.R. Chae, A. Drews, M. Kraume, H.S. Shin, F. Yang, Recent advances in membrane bioreactors (MBRs): membrane fouling and membrane material, *Water Res.* 43 (6) (2009) 1489–1512.
- [29] W. Lee, S. Kang, H. Shin, Sludge characteristics and their contribution to microfiltration in submerged membrane bioreactors, *J. Membr. Sci.* 216 (1–2) (2003) 217–227.
- [30] S. Rosenberger, C. Laabs, B. Lesjean, R. Gnirss, G. Amy, M. Jekel, J.-C. Schrotter, Impact of colloidal and soluble organic material on membrane performance in membrane bioreactors for municipal wastewater treatment, *Water Res.* 40 (2006) 710–720.
- [31] P. van den Brink, O.-A. Satpradit, A. van Bentem, A. Zwijnenburg, H. Temmink, M. van Loosdrecht, Effect of temperature shocks on membrane fouling in membrane bioreactors, *Water Res.* 45 (15) (2011) 4491–4500.
- [32] W. Guo, H.-H. Ngo, S. Vigneswaran, F. Dharmawan, T.T. Nguyen, R. Aryal, Effect of different flocculants on short-term performance of submerged membrane bioreactor, *Sep. Purif. Technol.* 70 (3) (2010) 274–279.
- [33] H. Koseoglu, N. Yigit, V. Iversen, A. Drews, M. Kitis, B. Lesjean, M. Kraume, Effects of several different flux enhancing chemicals on filterability and fouling reduction of membrane bioreactor (MBR) mixed liquors, *J. Membr. Sci.* 320 (1–2) (2008) 57–64.
- [34] P. Le-Clech, V. Chen, T.A.G. Fane, Fouling in membrane bioreactors used in wastewater treatment, *J. Membr. Sci.* 284 (1–2) (2006) 17–53.